35th Annual International Conference of the IEEE EMBS
Osaka, Japan, 3 - 7 July, 2013

Study of Neurovascular Coupling Functions for Transient Focal Cerebral Ischemia in Rats using Electrocorticography Functional Photoacoustic Microscopy (ECoG-fPAM)

Lun-De Liao[+*], Meng-Lin Li[+], Hsin-Yi Lai, You-Yin Chen and Nitish V. Thakor
*E-mail: gs336.tw@gmail.com

***Abstract*—Recently, the functional photoacoustic microscopy (fPAM) system has been proven to be a reliable imaging technique for measuring the total hemoglobin concentration (HbT), cerebral blood volume (CBV) and hemoglobin oxygen saturation (SO_2) in single cerebral blood vessels of rats. In this study, we report for the first time the combination of electrocorticography (ECoG) recordings and fPAM (ECoG-fPAM) to investigate functional hemodynamic changes and neuro-vascular coupling in single cortical arterioles of rats with electrical forepaw stimulation after photothrombotic stroke. Because of the optical focusing nature of our fPAM system, photo-induced ischemic stroke targeting on single cortical arterioles can be easily conducted with simple adaptation. Functional cerebral HbT, CBV and SO_2 changes associated with the induced stroke in selected arterioles from the anterior cerebral artery system were imaged with a 36 × 65-μm spatial resolution. The ECoG-fPAM system complements existing imaging techniques and has the potential to offer a favorable tool for explicitly studying cerebral hemodynamics and neuro-vascular coupling in small animal models of photo-induced ischemic stroke.**

***Keywords*— Photothrombotic stroke, Functional photoacoustic microscopy, Cerebral hemodynamic response, Forepaw electrical stimulation, Electrocorticography (ECoG), Somatosensory-evoked potentials (SSEPs).**

I. Introduction

Notably, *in vivo* optical imaging techniques, for example, diffusion optical imaging (DOI) [1] and laser speckle imaging (LSI) [2], have been increasingly used to study brain function [3]. These techniques can assess oxy- and deoxy-hemoglobin (i.e., HbO_2 and Hb) through their distinctive optical absorption characteristics [4-7]. The DOI technique is capable of assessing changes in CBV, HbO_2 and Hb in mice in response to peripheral stimuli through intact skulls [8]. However, for DOI, light scattering from tissue and the nonlinear relationship between the detected signal intensity and absorption coefficients make quantification of SO_2 problematic [9, 10] and also complicate the visualization of hemodynamic changes in single blood vessels. By contrast, LSI can probe cerebral hemodynamic changes in single blood vessels with high spatial resolution when the skull is removed [11]. However, due to the naturally limited penetration depth and poor resolution of LSI, it only can probe information from the single vessels that reflect the cortical cerebral surface; no depth information on a single blood vessel can be provided by LSI [2, 12, 13].

Functional photoacoustic microscopy (fPAM), which can measure functional hemoglobin changes in single vessels without the use of a label, is ideal for *in vivo* imaging of changes in HbT, CBV and SO_2 [14]. Recently, PA imaging has been reliably used in the following applications: breast tumor detection [15], oxygenation monitoring in blood vessels [14, 16], subcutaneous vasculature imaging [17] and neurovascular coupling imaging [18-21]. Based on a block design paradigm and multi-wavelength PAM, we first proposed a functional analysis method to image qualitative changes in HbT and SO_2. The current fPAM system has been used to image hemodynamic changes in specific cortical regions of the brain but not in specific blood vessels [19].

Recently, we reported for the first time that the regulation of functional HbT, CBV, and SO_2 changes in single cerebral blood arterioles can be reliably studied using the current fPAM system without the use of contrast agents [20].

In this study, for the first time, fPAM techniques associated with electrocorticography (ECoG) recordings (ECoG-fPAM) were used to investigate functional changes in HbT, CBV, SO_2 and somatosensory evoked potentials (SSEPs) in specific single arterioles responding to left-forepaw stimulation using vessel-specific clotting by *in vivo* photothrombosis in rats. A continuous wave (CW) laser was used to trigger clotting in cortical single arterioles, and fPAM was then used to measure functional HbT, CBV, and SO_2 changes in the same arterioles

[+] Lun-De Liao and Meng-Lin Li contributed equally to this work.

Lun-De Liao* is with the Singapore Institute for Neurotechnology (SiNAPSE), National University of Singapore, Singapore. (E-mail: gs336.tw@gmail.com)

Meng-Lin Li is with the Department of Electrical Engineering, National Tsing Hua University, No. 101, Sec. 2, Kuang-Fu Rd., Hsinchu, Taiwan 300, R.O.C. (E-mail: mlli@ee.nthu.edu.tw)

Vassiliy Tsytsarev is with the Department of Anatomy and Neurobiology, University of Maryland School of Medicine, 20 Penn street, HSF-2, Baltimore, MD 21201, U.S.A (E-mail: tsytsarev@umaryland.edu)

Hsin-Yi Lai is with the Research Imaging Institute, University of Texas Health Science Center at San Antonio, 8403 Floyd Curl Drive, San Antonio, Texas 78229-3900, U.S.A (E-mail: happydry@ms36.hinet.net)

You-Yin Chen is with the Department of Biomedical Engineering, National Yang Ming University, No.155, Sec.2, Linong St., Taipei, Taiwan 112, R.O.C. (E-mail: youyin.chen@gmail.com)

Nitish V. Thakor is with the Singapore Institute for Neurotechnology (SiNAPSE), National University of Singapore, 28 Medical Drive, #05-COR, Singapore 117456 and Department of Biomedical Engineering, Johns Hopkins University, Traylor 701/720 Rutland Ave, Baltimore, MD 21205, U.S.A (E-mail: sinapsedirector@gmail.com)

and their neighboring and upstream arterioles after the single blood arterioles clotted. We studied the temporal dependence of the cerebral SSEPs and functional HbT, CBV and SO_2 changes in specific single arterioles and performed a comprehensive characterization of vascular dynamics during/after photothrombotic stroke. This ECoG-fPAM technique has the potential to increase our understanding of cerebral neurovascular functions and the ability to monitor cerebral functional changes in stroke in small animal models.

II. Materials and Methods

Electrocorticography-functional photoacoustic microscopy system (ECoG-fPAM)

The experimental setup of the novel fPAM includes 1) PA imaging, 2) photothrombotic stroke in single cortical blood vessels, 3) ECoG recordings and 4) current stimulation. The 50-MHz dark field confocal fPAM system was used to image functional changes in selected cortical blood vessels. Four-ns laser pulses were generated at a pulse repetition rate of 10 Hz by an optical parametric oscillator (Surlite OPO Plus, Continuum, USA), which was pumped by a frequency-tripled Nd:YAG Q-switched laser (Surlite II-10, Continuum, USA). Two visible wavelengths of the laser pulses, 560 and 570 nm (λ_{560} and λ_{570}), were employed for PA wave excitation [19]. The 50-MHz ultrasonic transducer used in the current fPAM system was custom-made by the Resource Center for Medical Ultrasonic Transducer Technology at the University of Southern California (http://bme.usc.edu/UTRC/). It has a -6 dB fractional bandwidth of 57.5%, a focal length of 9 mm and a 6 mm active element, offering an axial resolution of 36 μm and a lateral resolution of 65 μm [18]. ECoG signals were simultaneously measured on the same computer using a multichannel data acquisition system (Blackrock Microsystems, Salt Lake City, Utah, USA). Fluctuations in the laser energy were monitored with a photodiode (DET36A/M, Thorlabs, USA). The recorded photodiode signals were applied before any further signal processing to compensate for PA signal variations caused by laser-energy instability. The achievable penetration depth of the fPAM was 3 mm with approximately 18-dB SNR, where the SNR is defined as the ratio of the signal peak value to the root-mean-square value of the noise.

Animal Preparation

The Six male Wistar rats weighing 250–300 grams each were initially anesthetized with pentobarbital (50 mg/kg, intraperitoneally). The anesthetized rats were mounted on a custom-made acrylic stereotaxic head holder to reduce motion artifacts during the experiment, and the skin and muscle were cut away from the skull to expose the bregma landmark. The anteroposterior (AP) distance between the bregma and the interaural line [22] was directly surveyed. Next, three craniotomies were performed on each animal. A right-lateral cranial window of approximately 4 (horizontal) × 2 (vertical) mm was made with a high-speed drill. After the rat was secured to the stereotaxic frame and placed on the bed pallet, the pallet was moved into position at the bregma, which was 9 mm anterior to an imaginary line drawn between the center of each ear bar (the interaural line), as shown in Figure 1A.

The cortical blood vessels under the open-skull window of the rat cortical surface, indicated by solid red arrows in Figure 1B, were imaged *in vivo* by fPAM at λ_{570}, as shown in Figure 1C. In addition, the selected A1, A2 and A3 arterioles from the anterior segment of the forelimb somatosensory system can be observed in the projected C-scan image [23-25]. The anterior segment of the forelimb somatosensory system is also located within the anatomical borders of the primary somatosensory cortex that innervates the forepaw (S1FL) [25, 26]. Two epidural cortical electrodes were secured in the skull over the right-lateral S1FL cortex (coordinates from bregma: AP, -1.7 mm and -0.8 mm; ML, -4.5 mm) for ECoG recordings. A stainless steel screw was used as the reference electrode and positioned 2 mm caudal to lambda. Functional changes in HbT, CBV and SO_2 in these arterioles were imaged by fPAM scanning during stimulation or stroke conditions. These images were acquired along the black solid lines in the selected region shown in Figures 1B and 1D. Moreover, some branches of these blood vessels were also visualized in the projected C-scan image.

Single cortical vessels photothrombotic stroke procedure

Focal photothrombotic stroke was targeted to a single cortical arteriole within the right hemisphere forelimb somatosensory cortex (Figure 1A). An arteriole was selected based on its appearance and position within the anterior segment of the forelimb somatosensory map. To induce occlusion, we injected the photosensitizer Rose Bengal (Na^+ salt, R3877; Sigma), which was diluted to 10 mg/kg in Hepes-buffered saline, into the tail vein. Within 2 min of injection, an individual surface arteriole (n=6) was targeted for occlusion using 80 mW of 532 nm CW laser light (MGM-20; Beta Electronics. The CW laser light was coupled into the PA system's dark-field light path and strongly focused to a selected single surface arteriole. The targeted arteriole was illuminated for 5 min until a stable clot formed.

Forepaw electrical stimulation

Forepaw stimulation was applied to evoke functional hemodynamic changes in the cerebral vessels and was achieved by insertion of thin-needle stainless steel electrodes under the skin of the rat's left forepaw. Electrical stimulation was then applied with a stimulator (Model 2100, A-M Systems, USA). A monophasic constant current of four pulses of 6 mA intensity with a 0.2-ms pulse width at a frequency of 3 Hz and 10 s of stimulation duration were used. A block-design paradigm was employed in this study for functional signal acquisition. The selected 10 s stimulation duration was used to provide sufficient time for the hemodynamic response to reach a maximum value to enable the large amount of averaging necessary for analysis [27]. Each trial consisted of only one block, and the PA signals at λ_{560} or λ_{570} were acquired in this block to assess stimulation-induced hemodynamic changes in specific single cortical blood vessels. The SSEPs were also elicited by 10 s electrical stimulation of the forepaw and were recorded from epidural cortical electrodes. The timing used in our

block-design paradigm was adequate for the brain to recover back to the resting state before the next stimulus [19, 28].

Data analysis of SSEPs

The somatosensory-evoked potentials (SSEPs) induced by forepaw electrical stimuli were recorded before/after photothrombotic stroke. During 10 s recording sessions, the right-lateral SSEPs were filtered on pre-amp between 0.3-150 Hz and sampled at 1 kHz. The SSEPs from fPAM experiments were analyzed offline using MATLAB (MATLAB R12, Mathworks Inc., USA) to evaluate the evoked responses induced by forepaw electrical stimuli. The SSEP amplitudes of individual sweeps were averaged over 30 sweeps to generate an averaged SSEP during the 200 ms post-stimulus period. Afterward, the averaged SSEP was subdivided into the two most commonly observed SSEP components: P1 (the first maximum voltage after stimuli) and N1 (the minimum voltage). The changes in SSEP components were used to evaluate the variations in the evoked responses induced by forepaw stimuli before/after photothrombotic stroke.

III. Results and Discussion

PA imaging of the cerebral vasculature

The relative positions of PA imaging and the open-skull window of the rat's right cortical surface are shown in Figures 1A and B. Blood vessels were observable on this cortical surface. The selected cerebral arterioles (i.e., A1, A2 and A3) [25, 26] and other blood vessels on the cortical surface could be observed visually, as indicated by block solid lines in Figure 1B. The vasculature of the cortex in the open window was imaged *in vivo* by fPAM at λ_{570}, as shown in Figure 1C. The selected cerebral arterioles in Figure 1C were imaged. In addition, some branches of these vessels were also visualized in the projected C-scan image (Figure 1C). An open-skull photograph of the brain surface was taken after stroke, as shown in Figure 1D. *In vivo* PA-projected C-scan images were acquired at λ_{570}. The blood vessels, as indicated by the red dashed circular lines in Figures 1B and 1C, are significant compared to the same positions in Figures 1D and 1E.

Stroke-induced functional PAM-measured CBV, HbT and SO_2 changes upon forepaw stimulation during and after photothrombotic stroke

The $I_{R(570)}$ images that were used to assess HbT changes in the A1, A2 and A3 arterioles are shown in Figure 2A; cases 1 and 2 are under normal conditions, and cases 3 through 9 are with stimulation after the onset of stroke. No significant HbT changes in the A1, A2 and A3 arterioles were observed in cases 1 and 2. In cases 3 through 9, with stimulation after stroke onset in case 3, significant HbT changes were observed in the A1 and A3 arterioles contralateral to the left-forepaw electrical stimulation. In contrast, reducing HbT changes were observed in the A2 arteriole. Comparing cases 3 through 9 under only the stimulation condition in the A1 and A3 arterioles, only case 3 exhibited significant HbT, CBV and SO_2 changes, but no significant HbT, CBV and SO_2 changes were observed in cases 4 through 9, even after stroke. Moreover, a significant reduction in HbT, CBV and SO_2 was observed in the A2 arteriole. The maximum HbT, CBV and SO_2 changes in case 3 under stimulation after stroke were 2.84, 1.28 and 2.32 ± 0.001 (mean ± SD), respectively. In cases 4 through 8 under the stroke condition, the averaged changes in HbT in the A1, A2 and A3 arterioles were 1.42, -6.48 and 1.77 ± 0.001 (mean ± SD), respectively. In addition, the averaged changes in SO_2 in the A1, A2 and A3 arterioles were 1.16, 0.21 and 1.22 ± 0.001 (mean ± SD), respectively. The averaged changes in $-R_{SO_2}$ in the A1, A2 and A3 arterioles were 1.32, -6.15 and 1.56 ± 0.001 (mean ± SD), respectively.

ECoG recordings during and after photothrombotic stroke

The waveforms of the averaged SSEPs over the recording sessions are shown in Figure 2B. Two main SSEP components labeled at the waveform were consistently observed: 1) P1, a peak-patency surface-positive component and 2) N1, a longer latency surface negativity. These two SSEP components (P1 and N1) are the best indices for comparing our PA imaging for probing cerebral hemoglobin responses. Significant differences in SSEP amplitudes were observed before and after photothrombotic stroke under the same intensity of forepaw stimuli. The peak-latency of P1 and N1 appeared at 16.5±0.15 ms and 23.5±0.49 ms, respectively, during the 200-ms post-stimulus period before the photothrombotic stroke. After induction of photothrombotic stroke, the peak-latency of P1 and N1 appeared at 18.31±0.16 ms and 27.49±0.45 ms during the 200-ms post-stimulus period, respectively.

IV. Conclusions

The present study is the first to demonstrate the unique features of a novel ECoG-fPAM system in characterizing the responses of specific A1, A2 and A3 arterioles using vessel-specific clotting by *in vivo* photothrombosis in rats responding to left-forepaw stimulation. By comparing the fPAM and ECoG results, we confirmed the feasibility of using the fPAM technique to assess photothrombotic stroke in single blood vessels simultaneously with produced functional HbT, CBV and SO_2 changes at a resolution of 36 × 65 μm. The current fPAM-ECoG technique has potential for enabling an understanding of neurometabolic functions in single cortical blood vessels during/after brain stroke conditions and the elucidation of the corresponding unique physiological bases of other imaging techniques.

Figures

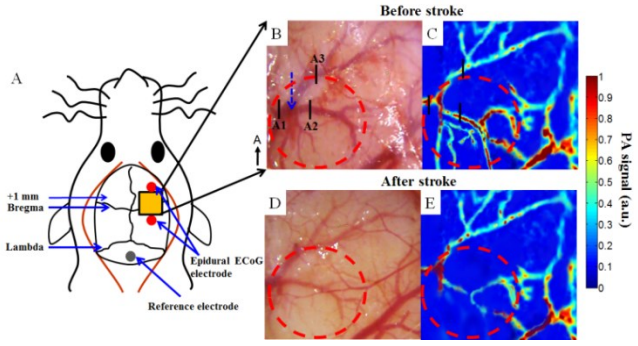

Figure 1. (A) Position of the PA imaging area (yellow area), epidural ECoG electrodes (red circle) and reference electrode (gray circle) relative to the animal's head. (B) Open-skull photograph of the cerebral cortical surface, as enlarged along the solid line from (A). The block solid lines in (B) indicate the selected cortical A1 (upstream), A2 (occluded blood vessel) and A3 (neighboring) arterioles that were studied. The blue dashed arrow indicates the position for photothrombotic stroke. The left black arrow points in the rostral direction. (C) *In vivo* PA-projected C-scan image of the cortical blood vessels in the superficial layer of the cortex, acquired at λ_{570}. (D) Open-skull photograph of the cortical surface after induction of stroke. (E) *In vivo* PA-projected C-scan image acquired at λ_{570} after the stroke.

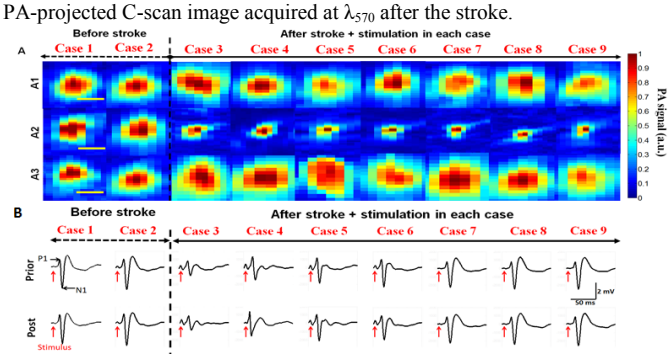

Figure 2. (A) *In vivo* PA cross-sectional B-scan images $I_{R(570)}$ of the cortical A1, A2 and A3 arterioles with stimulation from cases 3 through 9, after stroke onset in case 3. Significant HbT changes were observed only in the A1 and A3 arterioles. The yellow scale bars in the A1, A2 and A3 images denote 60 μm. (B) The waveforms and changes of the SSEP components before and after photothrombotic stroke. P1 and N1 are indicated by the first maximum voltage and the minimum voltage following forepaw stimuli, respectively.

References

[1] A. M. Siegel, J. P. Culver, J. B. Mandeville, and D. A. Boas, "Temporal comparison of functional brain imaging with diffuse optical tomography and fMRI during rat forepaw stimulation," *Physics in Medicine and Biology,* vol. 48, pp. 1391-1403, 2003.

[2] N. Li, X. Jia, K. Murari, R. Parlapalli, A. Rege, and N. V. Thakor, "High spatiotemporal resolution imaging of the neurovascular response to electrical stimulation of rat peripheral trigeminal nerve as revealed by in vivo temporal laser speckle contrast," *J Neurosci Methods,* vol. 176, pp. 230-236, 2009.

[3] V. Tsytsarev, C. Bernardelli, and K. I. Maslov, "Living brain optical imaging: technology, methods and applications," *J Neurosci Neuroeng,* vol. 1, 2012.

[4] D. Malonek and A. Grinvald, "Interactions between electrical activity and cortical microcirculation revealed by imaging spectroscopy : implications for functional brain mapping," *Science,* vol. 272, pp. 551-554, 1996.

[5] S. Prahl. (2007). *Optical Spectra*. Available: http://omlc.ogi.edu/

[6] L. V. Wang and H.-i. Wu, *Biomedical Optics: Principles and Imaging*: Wiley, 2007.

[7] E. M. C. Hillman, "Optical brain imaging in vivo: techniques and applications from animal to man," *Journal of Biomedical Optics,* vol. 12, pp. 051402-28, 2007.

[8] J. P. Culver, A. M. Siegel, M. A. Franceschini, J. B. Mandeville, and D. A. Boas, "Evidence that cerebral blood volume can provide brain activation maps with better spatial resolution than deoxygenated hemoglobin," *NeuroImage,* vol. 27, pp. 947-959, 2005.

[9] H. Dehghani, S. Srinivasan, B. W. Pogue, and A. Gibson, "Numerical modelling and image reconstruction in diffuse optical tomography," *Philosophical Transactions of the Royal Society A: Mathematical, Physical and Engineering Sciences,* vol. 367, pp. 3073-3093, 2009.

[10] G. Gratton and M. Fabiani, "Dynamic brain imaging: event-related optical signals (EROS) measures of the time course and localization of cognitive-related activity," *Psychonomic Bulletin and Review,* vol. 5, pp. 535-563, 1998.

[11] M. B. Bouchard, B. R. Chen, S. A. Burgess, and E. M. C. Hillman, "Ultra-fast multispectral optical imaging of cortical oxygenation, blood flow, and intracellular calcium dynamics," *Opt Express,* vol. 17, pp. 15670-15678, 2009.

[12] P. Miao, N. Li, N. V. Thakor, and S. Tong, "Random process estimator for laser speckle imaging of cerebral blood flow," *Opt Express,* vol. 18, pp. 218-236, 2010.

[13] M. Peng, A. Rege, L. Nan, N. V. Thakor, and T. Shanbao, "High resolution cerebral blood flow imaging by registered laser speckle contrast analysis," *IEEE Trans Biomed Eng,* vol. 57, pp. 1152-1157, 2010.

[14] L. V. Wang, "Multiscale photoacoustic microscopy and computed tomography," *Nat Photonics,* vol. 3, pp. 503-509, 2009.

[15] S. A. Ermilov, T. Khamapirad, A. Conjusteau, M. H. Leonard, R. Lacewell, K. Mehta, T. Miller, and A. A. Oraevsky, "Laser optoacoustic imaging system for detection of breast cancer," *J Biomed Opt,* vol. 14, p. 024007, 2009.

[16] H. F. Zhang, K. Maslov, G. Stoica, and L. V. Wang, "Functional photoacoustic microscopy for high-resolution and noninvasive in vivo imaging," *Nat Biotechnol,* vol. 24, pp. 848-851, 2006.

[17] H. F. Zhang, K. Maslov, and L. V. Wang, "In vivo imaging of subcutaneous structures using functional photoacoustic microscopy," *Nat Protoc,* vol. 2, pp. 797-804, 2007.

[18] L. D. Liao, C. T. Lin, Y. Y. Shih, T. Q. Duong, H. Y. Lai, P. H. Wang, R. Wu, S. Tsang, J. Y. Chang, M. L. Li, and Y. Y. Chen, "Transcranial imaging of functional cerebral hemodynamic changes in single blood vessels using in vivo photoacoustic microscopy," *J Cereb Blood Flow Metab,* Apr 4 2012.

[19] L.-D. Liao, M.-L. Li, H.-Y. Lai, Y.-Y. I. Shih, Y.-C. Lo, S. Tsang, P. C.-P. Chao, C.-T. Lin, F.-S. Jaw, and Y.-Y. Chen, "Imaging brain hemodynamic changes during rat forepaw electrical stimulation using functional photoacoustic microscopy," *NeuroImage,* vol. 52, pp. 562-570, 2010.

[20] L.-D. Liao, C.-T. Lin, Y.-Y. I. Shih, H.-Y. Lai, W.-T. Zhao, T. Q. Duong, J.-Y. Chang, Y.-Y. Chen, and M.-L. Li, "Investigation of the cerebral hemodynamic response function in single blood vessels by functional photoacoustic microscopy," *Journal of Biomedical Optics,* vol. 17, pp. 061210-10, 2012.

[21] S. Hu and L. V. Wang, "Neurovascular photoacoustic tomography," *Frontiers in Neuroenergetics,* vol. 2, p. 12, 2010-June-17 2010.

[22] G. Paxinos, Watson, Charles, *The rat brain in stereotaxic coordinates*. San Diego: Academic Press, 2007.

[23] M. H. Mohajerani, K. Aminoltejari, and T. H. Murphy, "Targeted mini-strokes produce changes in interhemispheric sensory signal processing that are indicative of disinhibition within minutes," *Proceedings of the National Academy of Sciences of the United States of America,* vol. 108, pp. E183-E191, May 31 2011.

[24] B. P. Chugh, J. P. Lerch, L. X. Yu, M. Pienkowski, R. V. Harrison, R. M. Henkelman, and J. G. Sled, "Measurement of cerebral blood volume in mouse brain regions using micro-computed tomography," *NeuroImage,* vol. 47, pp. 1312-1318, 2009.

[25] G. Paxinos, *The rat nervous system*, Third Edition ed., 2004.

[26] R. Weber, P. Ramos-Cabrer, C. Justicia, D. Wiedermann, C. Strecker, C. Sprenger, and M. Hoehn, "Early Prediction of Functional Recovery after Experimental Stroke: Functional Magnetic Resonance Imaging, Electrophysiology, and Behavioral Testing in Rats," *Journal of Neuroscience,* vol. 28, pp. 1022-1029, 2008.

[27] J. B. Mandeville, J. J. Marota, C. Ayata, M. A. Moskowitz, R. M. Weisskoff, and B. R. Rosen, "MRI measurement of the temporal evolution of relative CMRO2 during rat forepaw stimulation," *Magnetic Resonance in Medicine,* vol. 42, pp. 944-951, 1999.

[28] K. J. Friston, P. Fletcher, O. Josephs, A. Holmes, M. D. Rugg, and R. Turner, "Event-related fMRI: Characterizing differential responses," *NeuroImage,* vol. 7, pp. 30-40, Jan 1998.